Postprint of: Lesiuk G., Junik K., Duda S., Socha T., Kula K., Denisiewicz A., Medyński D., Macek W., Correia J. A., Prediction of the fatigue lifetime of PUR structural elements using a combined experimental-numerical approach, Structures, Vol. 59 (2024), 105822, DOI: 10.1016/j.istruc.2023.105822

Prediction of the fatigue lifetime of PUR structural elements using a combined experimental-numerical approach

Grzegorz LESIUK[1], Krzysztof JUNIK[1], Szymon DUDA[1], Tomasz SOCHA[2], Krzysztof KULA[2], Arkadiusz DENISIEWICZ[2], Daniel MEDYŃSKI[3], Wojciech MACEK[4], José CORREIA[5]

[1] Wroclaw University of Science and Technology, Faculty of Mechanical Engineering, Wroclaw, Poland

2 University of Zielona Góra; The Faculty of Civil Engineering, Architecture and Environmental Engineering, ul. prof. Z. Szafrana 1 PL65516 Zielona Góra, Poland T.Socha@ib.uz.zgora.pl, K.Kula@ib.uz.zgora.pl, A.Denisiewicz@ib.uz.zgora.pl

3 Witelon Collegium State University, Department of Production Engineering and Logistics, Faculty of Technical and Economic Sciences, Sejmowa 5A, 59-220 Legnica, Poland

4 Gdansk University of Technology, Faculty of Mechanical Engineering and Ship Technology, 11/12 Gabriela Narutowicza, Gdansk 80-233, Poland

5 CONSTRUCT & INEGI, University of Porto, Rua Dr. Roberto Frias, 4200-465 Porto, Portugal

Emails: Grzegorz.Lesiuk@pwr.edu.pl; kj@strongflex.eu; Szymon.duda@pwr.edu.pl; T.Socha@ib.uz.zgora.pl; K.Kula@ib.uz.zgora.pl; A.Denisiewicz@ib.uz.zgora.pl; daniel.medynski@collegiumwitelona.pl; wojciech.macek@pg.edu.pl; jacorreia@fe.up.pt

***Corresponding author:** jacorreia@fe.up.pt

ABSTRACT.

This paper presents a method for estimating the fatigue life of polyurethane elastomeric components. A rubber replacement - polyurethane of hardness 80ShA commonly used in vibration damping systems, for example, in motor vehicle suspensions, was used for the study. A metal-rubber bushing component was selected for analysis, and numerical analysis was carried out along with a fatigue model proposal based on a modification of the Wang-Brown model. The results obtained indicate that the description of the durability process using the proposed relationship is also possible. A constitutive model based on Ogden's hyperelastic model was identified and verified. The proposed methodology can be used in any part analysis based on the numerical model and fatigue data. The paper also evaluates the effectiveness of other models against the proposed relationship.

Keywords: Fatigue behavior, rigid PUR, FEA, Fatigue lifetime prediction.

Nomenclature

α	- Experimentally determined constants
α_i	- Temperature-dependent material parameters
$\Delta\gamma$	- Shear strain range
$\Delta\varepsilon_n$	- Normal strain range
$\bar{\lambda}_i$	- Deviatoric principal stretches
σ_n	- Normal stress acting in the critical plane,
σ_c	- Critical rupture stress
θ	- Critical plane position angle of the plane
μ_i	- Shear modulus
BM	- Brown-Miller criterion
D_i	- Incompressible parameter
K_0	- Bulk modulus
JWB	- Junik-Wang-Brown model
PUR	- Polyurethane
RP	- Reference point
S	- Experimentally determined constants
ShA	- Shore A Hardness Scale
N	- Order of the model
WB	- Wang-Brown model

1. Introduction

Polyurethane (PUR) is a widely used plastic with a variety of properties and functionalities. It plays a key role in energy conservation in construction, transport, and food preservation. In modern homes and offices, they are widely used in the form of flexible foam. The furniture made of it is soft and, at the same time, sufficiently durable, keeping its shape. Polyurethane foams fill seats and mattresses, and the possibility of using different material densities ensures high application potential. The flexible foams follow the shape of the body and support it, maintaining the correct posture when sitting and lying down. Polyurethane is perfectly suited for use as a component of modern furniture coatings, automotive and rail vehicles, power cables, floors, walls, roads, and bridges. Due to its properties, it protects exposed surfaces against the negative influence of pollution and environmental factors. Durability, corrosion resistance, and weather conditions make polyurethane suitable for covering various types of surfaces.

Polyurethanes are also interesting as a composite material for various applications [1], [2] including mining machinery [3] and the automotive industry [4] as replacement for rubber materials. Typically, PUR with the 80 in Shore scale A is a material used as a conventional rubber-like hardness in a suspension system. Elastomers represent a highly non-linear elastic material with large deformations. Their behavior is complex and dependent on many factors, such as the crosslinking state, loading conditions, the stress softening effect (also called Mullins effect), and time-dependent effects [5]. PUR materials have excellent energy absorption and dynamic damping capabilities [6].

The aforementioned complexity of the behavior forces engineers and scientists to make an effort to reflect the mechanical performance of the material properly. There are already some modelling approaches that estimate static mechanical behavior, such as the Ogden, Mooney-Rivlin, Yeoh, or Kilian model [7]. The pioneering work in the mathematical description of rubber materials (and thus elastomers) is the work of Mooney [8] and Rivlin [9]. They demonstrated that the commonly used linear theory and Hooke's law is are inadequate tool to describe hyperelastic materials. It was not until the development of the idea of elasticity in the range of large deformations that contributed, among others, thanks to the work of [10]–[12] to a better description and understanding of the mechanics of elastomeric materials. The authors have extensively researched the applicability of fracture mechanics and static modeling of PUR material using available models in papers [13]–[15]

The nature of polyurethane component loading requires a comprehensive analysis of behaviour under static and cyclic loading conditions defined by the application. Since static behaviour can be reasonably described by the models above and is proved in the previous article by the authors [15], it is not the main objective of this investigation. Thus, the focus is placed on the fatigue lifetime estimation of the components made from PUR material.

The state-of-the-art presented in [16]–[18] shows that several fatigue modelling approaches can be found in the scientific literature and can be grouped for crack nucleation and the crack growth approach. This division reflects the general manner of fracture of elastomers under cycling load. Such materials often fail due to crack nucleation (initiation phase) and their growth. Within the first approach group, criteria can be found based on the maximum principal strain and strain energy density. On the other hand, the energy release rate is introductory in analysing the propagation phase. Of the available approaches, only two proposed by Brown et al. [19], [20] are considered and modified to assess the useful life of the PUR component subjected to cycling load. Evaluation of fatigue life is crucial from a design perspective. A properly calibrated fatigue model can assess the durability of the designed element. Simultaneously, it increases safety and reduces the required experimental campaign.

This research concerns the experimental–numerical fatigue lifetime assessment of PUR components used in vehicle suspension subjected to complex loading conditions. Presented within the investigation, the modified fatigue model shows off the innovative nature of the manuscript.

2. Materials and Methods

This section includes all necessary information about the material, specimens, and conducted experimental tests. The research framework is shown in the flow chart form in Figure 1.

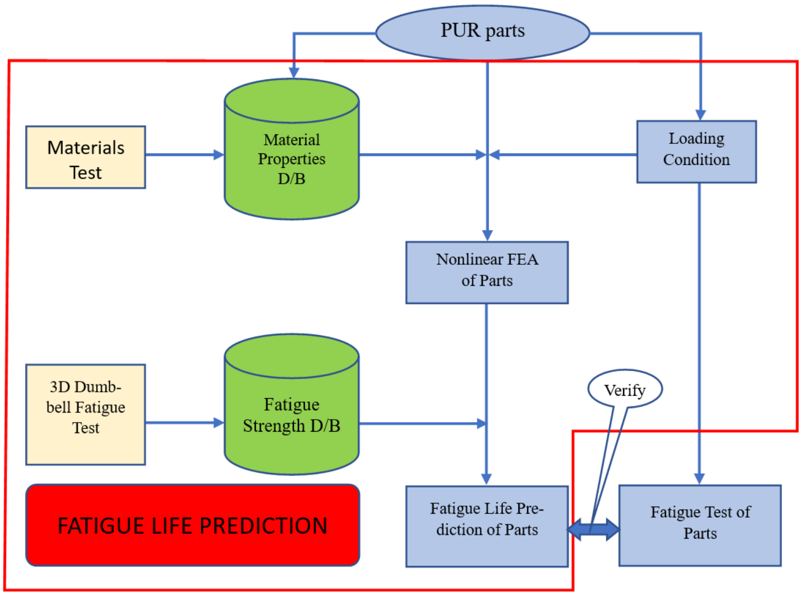

Figure 1 Flow chart of the proposed fatigue lifetime analysis of components

Analysis has been done for a polyurethane metal bushing commonly used in vehicle suspension systems. A technical drawing of the component is shown in Figure 2. As was mentioned before, commonly used for such an application is PUR material with a hardness of 80 on a Shore A scale. This material is a substitute for rubber parts. However, PUR material exhibits greater durability with respect to rubber-made parts. Due to cost, it is used mainly in sport vehicles, where performance is significantly more important than cost.

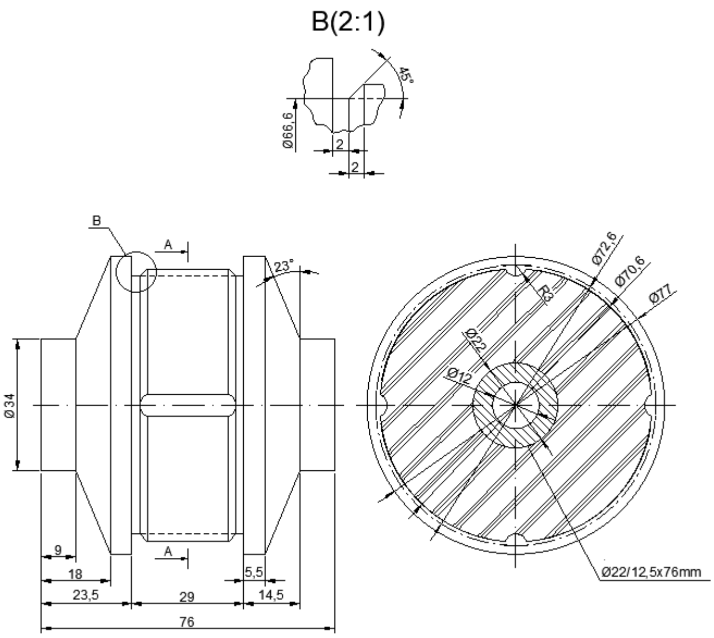

Figure 2 Scheme and dimensions of the components designed for the fatigue test (dimensions in mm).

Experimental procedure

Fatigue tests were carried out on an MTS 810 testing machine using a specially designed clamping system to simulate the conditions in service in the suspension system. An example of a component manufactured for testing (80 ShA) and a designed gripping system is shown in Figure 3. The specimen was loaded with a force amplitude of 20 kN, 15 kN, and 10 kN, respectively, at a frequency of 1 Hz to avoid the temperature effect. For this purpose, temperature was monitored periodically using thermal imaging cameras – FLIR TGXXX series. During the experiment, the proper phase of fatigue testing, the temperature span does not exceed 25°C for a wide range of strain levels. As in the case of test interruption, more than a 50 % drop in specimen stiffness was used as the stop criterion.

The validation of the raw PUR material was confirmed by the tensile test performed according to ASTM D412 [21] using flat dumbbell samples of 2 mm thickness. Based on the experimental results, a numerical model was performed to analyze the strains and stresses that act on the components tested. It was fundamental to determine and estimate fatigue life.

Figure 3 Specimen during fatigue test (80 ShA)

3. Experimental results and numerical modeling

Initially, it was necessary to verify the tensile properties of the used PUR material. It is fundamental for the calibration of models. It was already done by the authors and presented in [15]. Table 1 gives the data obtained for the static tensile test.

Table 1 Analysis of the results of the tensile test for the 80 ShA material configuration

SPECIMEN ID	UTS - Ultimate Tensile Strength (MPa)	A – elongation at break (%)
PU80_#1	17.9	749.2
PU80_#2	19.4	646.4
PU80_#3	21.6	651.0
PU80_#4	19.0	710.4
PU80_#5	23.7	711.0

Subsequently, the fatigue tests were performed and plotted in terms of the S-N curve fitted using linear regression, which is performed by means of power law. The results of the fatigue test are shown in

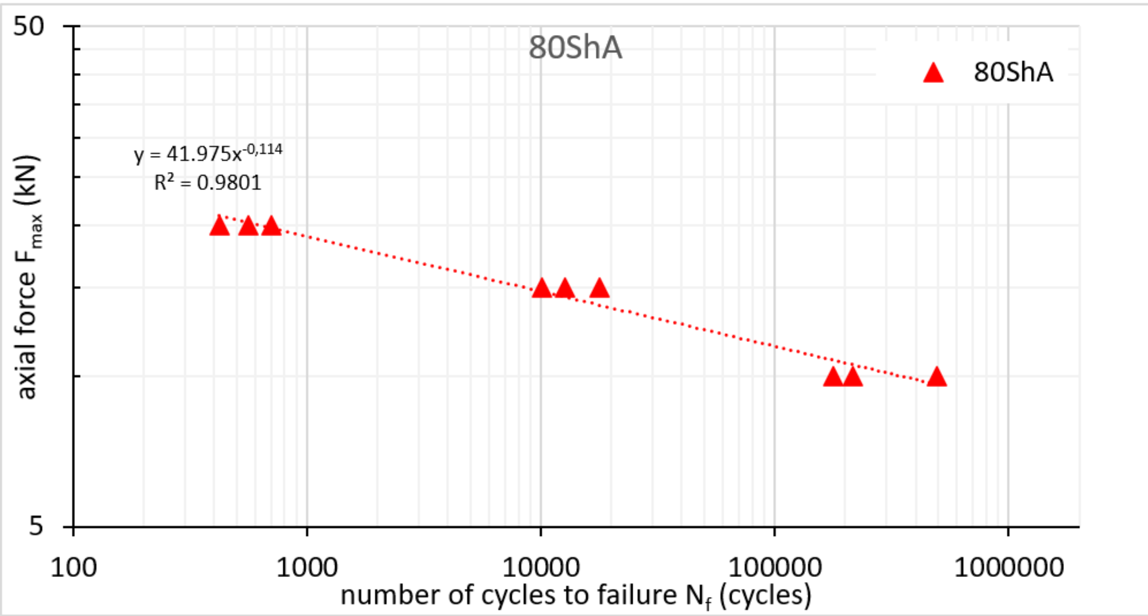

Figure 4 Fatigue curve obtained for 80 ShA polyurethane bushes (based on [22]*)*

The samples after fatigue tests are shown in Figure 5 – 6. Figure 5 presents a damaged component after N_f = *approximately* 170 thousand cycles [22]. A large major longitudinal crack is evident. Another damage mechanism (80 ShA) is shown in Figure 6 and is dominated by ductile deformation, corresponding to F_{max} = 20 kN [22]. An important conclusion from the observations was that the location of the damage plane was identified. This plane included the location of the main crack that led to fatigue failure.

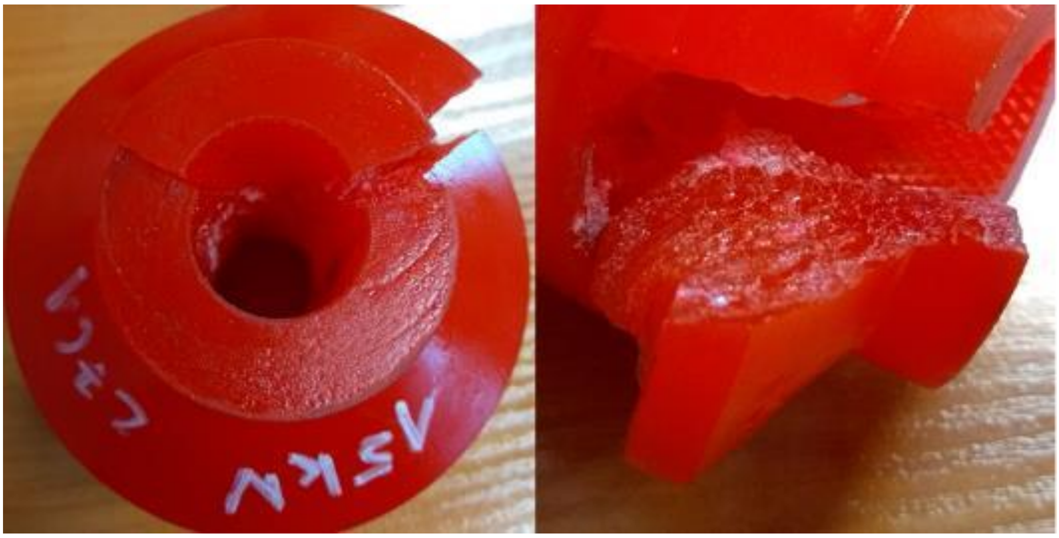

Figure 5 Damaged 80 ShA polyurethane sample (load level 15kN)

Figure 6 Damaged 80 ShA polyurethane sample (load level 20kN)

The fracture nature observed under service conditions is used to assess the results obtained by numerical analysis, performed simultaneously.

Numerical analysis

Commercially available finite element software offers a tool for model calibration. Several models are available in the software. Based on the results and detailed analysis conducted by the authors in [15]. The Ogden material model was chosen and calibrated because it reflects the mechanical behavior with the highest precision under tension load. The Ogden [23] model is a very general hyperelasticity model with a Helmholtz free energy per reference volume that is expressed in terms of the principal stretches applied and presented in Eq. (1).

$$W = \sum_{i=1}^{N} \frac{2\mu_i}{\alpha_i^2}\left(\bar{\lambda}_1^{\alpha_i} + \bar{\lambda}_2^{\alpha_i} + \bar{\lambda}_3^{\alpha_i} - 3\right) \tag{1}$$

Where $\bar{\lambda}_i$ denote the deviatoric principal stretches. N – order of the model. μ_i, α_i temperature-dependent material parameters. The initial shear modulus and the bulk modulus are given by:

$$\mu_0 = \sum_{i=1}^{N} u_i,\ K_0 = \frac{2}{Di} \tag{2}$$

The calibration procedure was described in the previous article of the authors [24], for 80 ShA material, the Ogden model with 3 model parameters fits the appropriate parameters presented in Table 2.

Table 2 Ogden model parameters for 80ShA

	$\boldsymbol{\mu_i}$	$\boldsymbol{\alpha_i}$
1	4.34400372	-0.380731347
2	0.210081339	3.47276528
3	4.921467147E-03	-6.93803394

Moreover, the stability assessment says that the model is stable for the entire range of strains in each test (uniaxial, biaxial, planar, volumetric). Further analysis concerns the comparison of the obtained FEM numerical results with the experimental results. The uniaxial test was conducted to provide a force vs. displacement relationship. The test was carried out on the MTS Bionix hydraulic testing machine system with a 50 mm/min displacement control mode. The numerical results show good agreement with the experimental data, as presented in Figure 7.

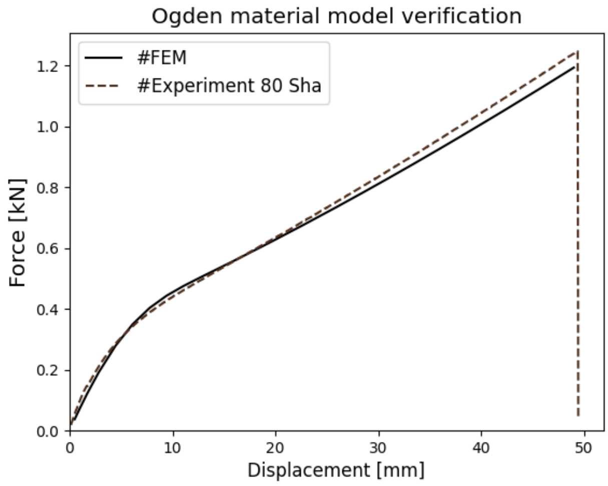

Figure 7 Comparison of the results obtained from numerical simulation and experiment

A 3D solid geometry represents a numerical model of the PUR bushing according to Figure 8. Finite element analysis was performed using Abaqus software in a static term. The model consists of two sub-parts, respectively: bushing made from PUR 80 ShA, and cylindrical insert made from steel S235 Figure 8. The previously defined PUR material model was applied, where, for steel, the following elastic properties presented in Table 3 were used.

Table 3 Typical elastic properties of S235 steel

	E	**Poisson's ratio**
Steel S235	210 GPa	0.3

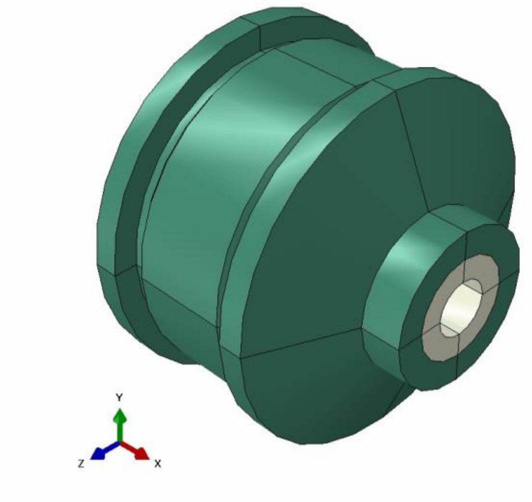

Figure 8 Geometry of the analyzed assembly made of PUR material (green section) with steel insert (gray section)

The purpose of this FE modeling is to obtain the distribution of the stress hot spots and to calculate the stress and strain tensor components in the critical plane position for the following loads: 10 kN, 15 kN, and 20 kN. The following boundary conditions shown in Figures 9 - 10 were applied to provide such loading conditions. The load transfer to the sample is carried out by coupling the reference points to the inner surfaces of the steel insert (Figure 9). The outer surface of the bushing was used to provide fixed support (translation and rotation in all three directions are pinned), and the load is provided by a displacement boundary condition applied to the reference point (RP-1) (Figure 10).

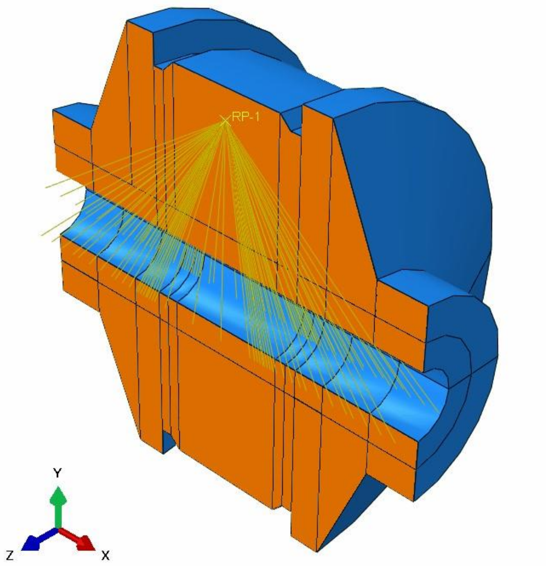

Figure 9 Representation of boundary conditions applied to the specimen - coupling connection of the reference point

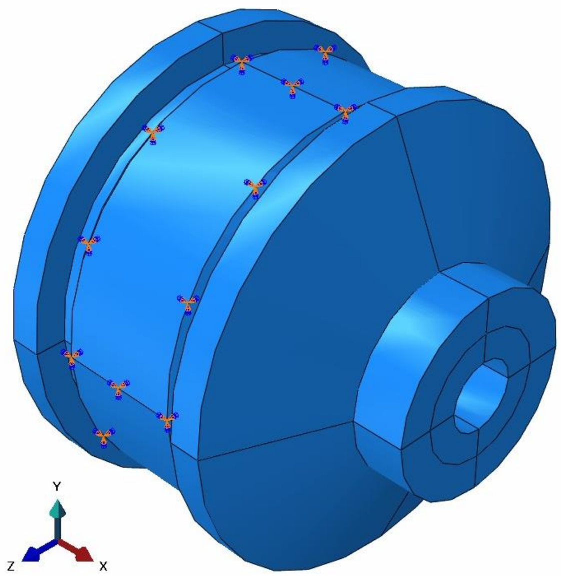

Figure 10 Representation of boundary conditions applied to the specimen, fixed support.

The presented geometry with the applied loading conditions was merged into a finite continuum object. The mesh applied to the object consists of 40 356 quadratic hexahedral elements of type C3D20H. The set of element sizes for this model is 1.5 mm; however, some regions were enriched with additional nodes. Figure 11 shows the final meshed geometry; other areas with the most nodes are noticeable. This enhanced region allowed one to obtain more adequate results.

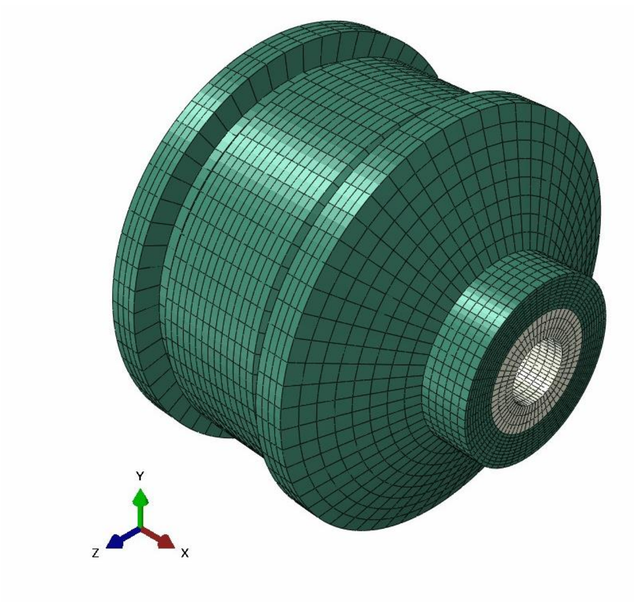

Figure 11 Discrete model of the bushing system.

An exemplary principal stress distribution is shown in Figure 12. As it is noticeable, the local concentration appears below the outer surface. Those spots may suggest the vicinity of the crack nucleation.

a) *b)*

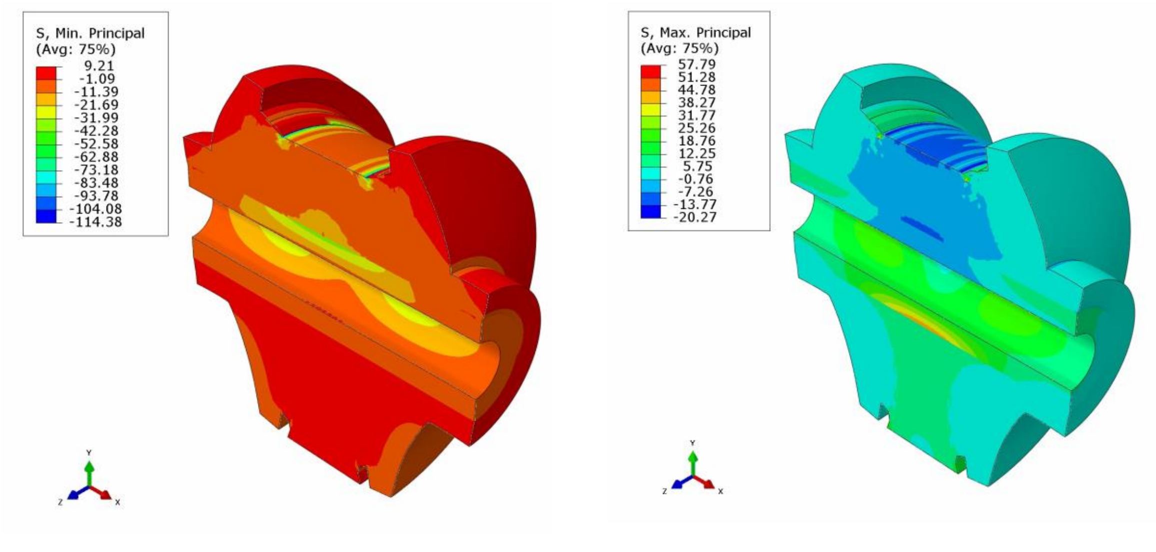

Figure 12 Minimum (a) and maximum (b) principal stress distribution for 80 ShA – load case 20kN (in MPa)

Having a closer look at the fracture plane defined during the fatigue experiment, the crack nucleation given by finite element analysis seems to be of great probability. A comparison is provided and similarities can be found in Figure 13.

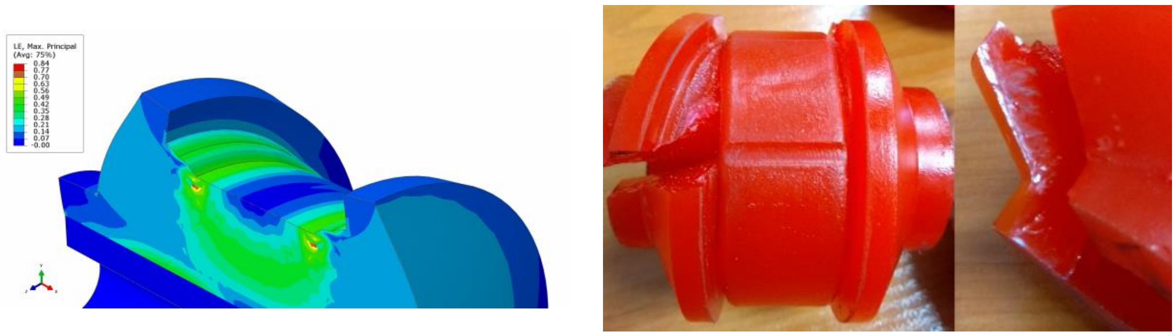

Figure 13 Comparison of results along the experiment and analysis of finite elements. Numerical results present the logarithmic strain components at the integration points (unitless).

4. Fatigue lifetime prediction and discussion

The calculations were carried out in two ranges:

- First approach based on the peak strain / stress component, uniaxial loading,
- Second approach considering multiaxial loading and current stress/strain state in the damage zone.

The first approach requires only the maximum strain values as a main predictor of fatigue damage. On the other hand, to analyze the strain state, it was necessary to use commonly used criteria for multiaxial fatigue damage. The most popular Brown-Miller (BM) criterion [20]:

$$BM = (\Delta\gamma_{max}{}^{\alpha} + S\Delta\varepsilon_n{}^{\alpha})^{\frac{1}{\alpha}} \tag{2}$$

where:

BM – is an equivalent strain value,

$\Delta\gamma$ – shear strain range,

$\Delta\varepsilon_n$ – is the normal strain range,

α, S – experimentally determined constants.

The BM criterion was based on the maximum shear stress plane. Another evolution of the BM model was the Wang-Brown (WB) modification, which allowed applications of the concept of a critical plane concept [19]

$$WB = max_{\theta}\left(\frac{\Delta\gamma}{2} + S\Delta\varepsilon_n\right) \tag{3}$$

where:

θ - critical plane position angle of the plane.

As it seems, finding the experimental parameters - in particular the BM and WB - *S* parameters - has resulted in a multidimensional, nontrivial issue. In addition, there is not enough guidance on identifying this parameter in the literature. For its estimation, mathematical estimation was used by fitting the model to the experimental data. In the calculations, a constant value of *S*=0.25 was assumed. On the other hand, observing the experimental data led to the modification and results in the JWB - Junik-Wang-Brown approach. The revision proposed by the authors is given by Eq. (4).

$$JWB = max_{\theta}\left(\frac{\Delta\gamma}{2} + \frac{\sigma_n}{\sigma_c}\Delta\varepsilon_n\right) \tag{4}$$

where:

σ_n – normal stress acting in the critical plane,

σ_c – critical rupture stress.

The effectiveness of the strain approach (based on the peak strain concept), WB and JWB models for polyurethane materials, is shown in Figure 14, where the predictions are presented. Analysis of both graphs shows that forecasts based only on the uniaxial strain criterion are entirely incorrect. Moreover, the results obtained are underestimated and therefore not conservative, which can be particularly dangerous in the context of operation. The WB criterion correctly predicts fatigue life, resulting in five points for 80 ShA that fall outside the lifetime factor ×2 and all matters within the lifetime factor ×3. In contrast, the JWB criterion proposed in this dissertation predicts fatigue life much better, resulting in 80 ShA having only one point outside the lifetime factor ×2 and all points within the lifetime factor ×3. The fundamental advantage of the JWB model is that, for the materials tested, each time it only required knowledge of the static strength parameters without having to mathematically 'estimate' the value of the *parameter S.*

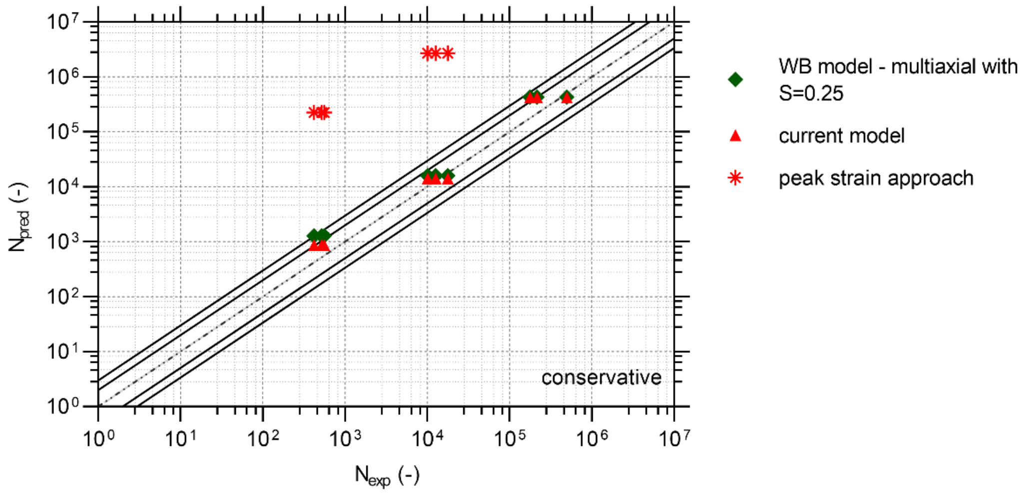

Figure 14 Predictions results for the 80 ShA component

5. Conclusions

The fatigue life assessment presented in the following research was based on experimental (static and fatigue tests) and numerical analysis. The calibration procedure for the material's models of suspension bushing made from PUR 80 ShA was performed. At the same time, finite element analysis was performed to obtain strains during fatigue loading. Based on that, it allows draw the following conclusions.

- The behaviour of the two polyurethane elastomeric materials with different harnesses can be successfully described by Ogden's constitutive model (N=3, 4).
- For bushing system peak strain approach in fatiguelifetime analysis is insufficient,
- The proposed modification of the Wang-Brown model allows for more accurate fatigue life prediction (considering the multiaxial fatigue condition) of PUR components,
- On the contrary to the Wang-Brown model, better explanation of physical meaning constants S is dependent on the critical stress level and tensile properties.

Credit authorship contribution statement

Grzegorz Lesiuk: execution of the analytical study, data analysis, writing, supervision. **Krzysztof Junik**: execution of the analytical study, data analysis, writing. **Szymon Duda**: execution of the analytical study, data analysis, writing. **Tomasz Socha**: data analysis, writing, validation. **Krzysztof Kula**: data analysis, validation, writing - review. **Arkadiusz Denisiewicz**: data analysis, validation, writing - review. **Daniel Medyński**: data analysis, validation, writing - review. **Wojciech Macek**: data analysis, validation, writing - review. **José Correia**: data analysis, validation, writing - review.

Declaration of competing interest

The authors declare that they have no known competing financial interests or personal relationships that could have appeared to influence the work reported in this paper.

Acknowledgements

The publication has been prepared as a part of the Support Programme of the Partnership between Higher Education and Science and Business Activity Sector financed by City of Wroclaw (Poland). This research was supported by base funding - UIDB/04708/2020 and programmatic funding - UIDP/04708/2020 of the CONSTRUCT - Instituto de I&D em Estruturas e Construções - funded by national funds through the FCT/MCTES (PIDDAC). José Correia would like to thank the individual project grant (2020.03856.CEECIND) awarded by national funds (PIDDAC) through the Portuguese Science Foundation (FCT/MCTES).

References

[1] M. Mrówka *et al.*, "The influence of halloysite on the physicochemical, mechanical and biological properties of polyurethane- -based nanocomposites," *Polimery*, vol. 65, no. 11–12, pp. 784–791, Dec. 2020, doi: 10.14314/polimery.2020.11.5.

[2] H. Taghipoor, A. Eyvazian, F. Musharavati, T. A. Sebaey, and A. Ghiaskar, "Experimental investigation of the three-point bending properties of sandwich beams with polyurethane foam-filled lattice cores," *Structures*, vol. 28, pp. 424–432, Dec. 2020, doi: 10.1016/J.ISTRUC.2020.08.082.

[3] M. Mrówka, M. Szymiczek, and J. Lenża, "Thermoplastic polyurethanes for mining application processing by 3D printing," *Journal of Achievements in Materials and Manufacturing Engineering*, vol. 95, no. 1, pp. 13–19, 2019, doi: 10.5604/01.3001.0013.7620.

[4] K. Junik, K. Snowacki, S. Duda, K. Towarnicki, and J. A. F. O. Correia, "Impact of hardness on the fracture and tear characterization of rigid pur materials used in suspension systems of vehicles," *Eng Fail Anal*, vol. 127, p. 105510, Sep. 2021, doi: 10.1016/J.ENGFAILANAL.2021.105510.

[5] J. Diani, B. Fayolle, and P. Gilormini, "A review on the Mullins effect," *Eur Polym J*, vol. 45, no. 3, pp. 601–612, Mar. 2009, doi: 10.1016/J.EURPOLYMJ.2008.11.017.

[6] Z. Zhao, X. Li, H. Jiang, X. Su, X. Zhang, and M. Zou, "Study on the Mechanical Properties and Energy Absorbing Capability of Polyurethane Microcellular Elastomers under Different Compressive Strain Rates," *Polymers 2023, Vol. 15, Page 778*, vol. 15, no. 3, p. 778, Feb. 2023, doi: 10.3390/POLYM15030778.

[7] S. K. Melly, L. Liu, Y. Liu, and J. Leng, "A review on material models for isotropic hyperelasticity," *International Journal of Mechanical System Dynamics*, vol. 1, no. 1, pp. 71–88, Sep. 2021, doi: 10.1002/MSD2.12013.

[8] M. Mooney, "A theory of large elastic deformation," *J Appl Phys*, vol. 11, no. 9, pp. 582–592, 1940, doi: 10.1063/1.1712836.

[9] R. S. Rivlin, "Large elastic deformations of isotropic materials IV. Further developments of the general theory," *Philosophical transactions of the royal society of London. Series A, Mathematical and physical sciences*, vol. 241, no. 835, pp. 379–397, 1948.

[10] R. W. Ogden, *Non-linear elastic deformations*. Courier Corporation, 1997.

[11] G. Holzapfel, "Nonlinear Solid Mechanics John Wiley & Sons," *Inc. Chichester*, 2000.

[12] W. M. Lai, D. H. Rubin, D. Rubin, and E. Krempl, *Introduction to continuum mechanics*. Butterworth-Heinemann, 2009.

[13] K. Junik, K. Snowacki, S. Duda, K. Towarnicki, and J. A. F. O. Correia, "Impact of hardness on the fracture and tear characterization of rigid pur materials used in suspension systems of vehicles," *Eng Fail Anal*, vol. 127, p. 105510, Sep. 2021, doi: 10.1016/J.ENGFAILANAL.2021.105510.

[14] P. Zielonka *et al.*, "Stress Relaxation Behaviour Modeling in Rigid Polyurethane (PU) Elastomeric Materials," *Materials*, vol. 16, no. 8, p. 3156, Apr. 2023, doi: 10.3390/ma16083156.

[15] K. Junik *et al.*, "Constitutive Law Identification and Fatigue Characterization of Rigid PUR Elastomers 80 ShA and 90 ShA," *Materials*, vol. 15, no. 19, p. 6745, Sep. 2022, doi: 10.3390/ma15196745.

[16] T. Gehling, J. Schieppati, W. Balasooriya, R. C. Kerschbaumer, and G. Pinter, "Fatigue Behavior of Elastomeric Components: A Review of the Key Factors of Rubber Formulation, Manufacturing, and Service Conditions," *Polymer Reviews*, vol. 63, no. 3, pp. 763–804, 2023, doi: 10.1080/15583724.2023.2166955.

[17] W. V. Mars and A. Fatemi, "A literature survey on fatigue analysis approaches for rubber," *Int J Fatigue*, vol. 24, no. 9, pp. 949–961, Sep. 2002, doi: 10.1016/S0142-1123(02)00008-7.

[18] W. V. Mars and A. Fatemi, “Factors that Affect the Fatigue Life of Rubber: A Literature Survey,” *Rubber Chemistry and Technology*, vol. 77, no. 3, pp. 391–412, Jul. 2004, doi: 10.5254/1.3547831.

[19] C. H. Wang and M. W. Brown, “A PATH-INDEPENDENT PARAMETER FOR FATIGUE UNDER PROPORTIONAL AND NON-PROPORTIONAL LOADING,” *Fatigue Fract Eng Mater Struct*, vol. 16, no. 12, pp. 1285–1297, 1993, doi: 10.1111/J.1460-2695.1993.TB00739.X.

[20] M. W. Brown and K. J. Miller, “A Theory for Fatigue Failure under Multiaxial Stress-Strain Conditions,” *Proceedings of the Institution of Mechanical Engineers*, vol. 187, no. 1, pp. 745–755, Jun. 1973, doi: 10.1243/PIME_PROC_1973_187_069_02.

[21] “D412 Standard Test Methods for Vulcanized Rubber and Thermoplastic Elastomers—Tension.” Accessed: Nov. 25, 2023. [Online]. Available: https://www.astm.org/d0412-16r21.html

[22] K. Junik *et al.*, “Impact of the hardness on the selected mechanical properties of rigid polyurethane elastomers commonly used in suspension systems,” *Eng Fail Anal*, vol. 121, Mar. 2021, doi: 10.1016/j.engfailanal.2020.105201.

[23] R. W. Ogden, “Large deformation isotropic elasticity–on the correlation of theory and experiment for incompressible rubberlike solids,” *Proceedings of the Royal Society of London. A. Mathematical and Physical Sciences*, vol. 326, no. 1567, pp. 565–584, 1972.

[24] K. Junik *et al.*, “Constitutive Law Identification and Fatigue Characterization of Rigid PUR Elastomers 80 ShA and 90 ShA,” *Materials*, vol. 15, no. 19, Oct. 2022, doi: 10.3390/ma15196745.